DOI: 10.47743/achi-2023-2-0009 *ACTA CHEMICA IASI*, **31_2**, 129-146 (2023)

SYNTHESIS, BACTERIAL INHIBITION, AND COORDINATION BEHAVIOR STUDY OF NEW AZOIMIDAZOLE LIGAND WITH SOME OF FIRST SERIES TRANSITION IONS

Israa N. Witwit[a], Husham M. Mubark[a], Zahraa Y. Motaweq[b], Mohauman M. Al Rufaie[a*]

[a]*Department of Chemistry, Faculty of Science, University of Kufa, Najaf, Iraq.*
[b]*Department of Biology, Faculty of Science, University of Kufa, Najaf, Iraq.*

Abstract: Coupling reaction between the diazonium salt of 3-chloro-4-fluoroaniline and 4-methyl imidazole used to create new Azoimidazole compound (4MCFD). Solid complexes of this ligand and series of transition metal ion were synthesized. The complexes and ligand were characterized by Mass Spectroscopy, ^{1}H-NMR,^{13}C-NMR, FT-IR, UV-Vis, Elemental Analysis, Molar Conductivity, and their inhibition ability against *E. coli, P. aeruginosa, K. pneumonia, and S. aureus* bacteria studied, according to the common chemical characterization methods. The values of stability constants were also calculated and showed high level of stability. All of the synthesized complexes have octahedral geometry with general formula $[M(4MCFD)_2Cl_2]$, (4MCFD) ligand behave as a bidentate. New ligand and its complexes exhibited significant inhibitory efficacy against gram-negative bacteria as compared to positive bacteria.

***Keywords*:** Azoimidazole, Bacterial, complexes, Inhibition, 4-methylimidazole, azo.

Introduction

Azoimidazoles are a class of heterocyclic azo coordination substances, which have recently garnered considerable attentions since they can serve as colorimetric reagents for various metal ions at their low

[*]Mohauman M. Al Rufaie, *e-mail:* muhaimin.alrufaie@uokufa.edu.iq

concentrations in the samples[1-3] and their flexibility to form a various coordination geometry.[4,5] Cylic azoimidazole ligands are considered the stable form of these compounds in which imidazole heterocyclic ring attached to azo group (-N=N-) from position 2 as shown in figure 1.

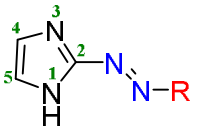

R= Hetero, or homocyclic ring

Figure 1. General structure of cyclic imidazole azo compounds.

The effective π-accepting ability of Azoimidazole ligands gave the coordination ability with metal ions at their low oxidation states.[6] The biological activity of these ligands and their coordination complexes, which also involves antimicrobial,[7-9] antitumor,[10] and antiviral properties, Furthermore, Azoimidazoles have been demonstrated to have antiviral activity by inhibiting the reproduction of several viruses, including the CVID1.[11,12] This ability promising attractive alternatives for the formation of new medications.

The aim of this study is preparing new Azoimidazole compound by coupling the reactions of 4-methyl imidazole and 3-chloro 4-floro aniline, characterize the new compound, studying coordination with varying divalent transition ions, and investigation. The antimicrobial activity of the free ligand and the complexes against some of bacterial resistance.

Experimental part

Chemical Materials

All of the solid, and liquid chemicals used for this study were supplied by BHD, Merck, Fluka, and AK Sentific companies and have high percentages of purity.

Instrumentation

Magnetic susceptibility for the purified solid complexes were recorded by Balance Magnetic Susceptibility Design - M.S. B Auto, Mass spectra were performed by SCIEX - 3200-Mass Analyzer.

^{1}H-NMR and ^{13}C-NMR spectra were measured by BRUKER Avance 300 Digital NMR, FT-IR measurements were caried by Shimadzu FTIR-8400S Spectrometer, Electronic spectrum measurements performed by a Shimadzu UV-1650 Spectrophotometer, whilst molar conductivity was measured by WTW inoLab pH/Cond 720. Elemental analysis (C.H.N) for the ligand and complexes were measured by Perkin Elmer 2400 Elemental Analyzer.

Synthesis of New (4MCFD) Ligand

(E)-2-((3-chloro-4-fluorophenyl) diazinyl)-4-methyl-1H-imidazole (4MCDF) was produced by mixing 10 mmol (1.45 g) of 3-chloro-4-fluoroaniline with 3 mL of hydrochloric acid in 30 mL of purified distilled water in an ice bath to keep the temperature between 0-5 ^{o}C, then gradually adding a solution of sodium nitrate 0.77 g in 10 mL of distilled water with continuously stirring. In alcoholic solution of 4-methyl imidazole prepared from the cold solution of 4-methyl imidazole by dissolving 10 mmol of diazonium salt (0.82 g) in 30 mL of ethanol in a basic medium, the diazonium salt solution was gradually added. Orange (4MCFD) precipitate formed, filtered, dried, and recrystallized from the hot ethanol as obvious in Scheme 1.

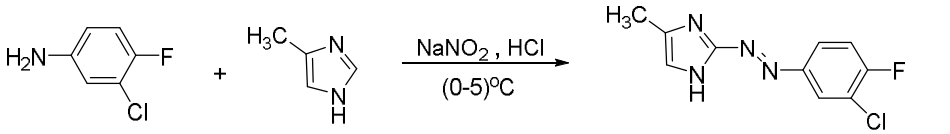

3-chloro-4-fluoroaniline 4-methyl-1H-imidazole (E)-2-((3-chloro-4-fluorophenyl)diazenyl)-4-methyl-1H-imidazole

Scheme 1. Synthesis equation of (4MCFD) ligand.

Preparation of (4MCFD) Solid Complexes

Solid complexes synthesized at 1 : 2 molar ratio (1 metal ion : 2 (4MCFD) ligand) by mixing 10 mmol of each $CoCl_2.6H_2O$, $NiCl_2.6H_2O$, $CuCl_2$, $CdCl_2$, and $HgCl_2$ salts with 20 mmol of (4MCFD) ligand in 25 mL of ethanol with continuous stirring until their precipitations appeared, then filtered and dried. The recrystallization process was done from hot ethanol, as shown in scheme 2.

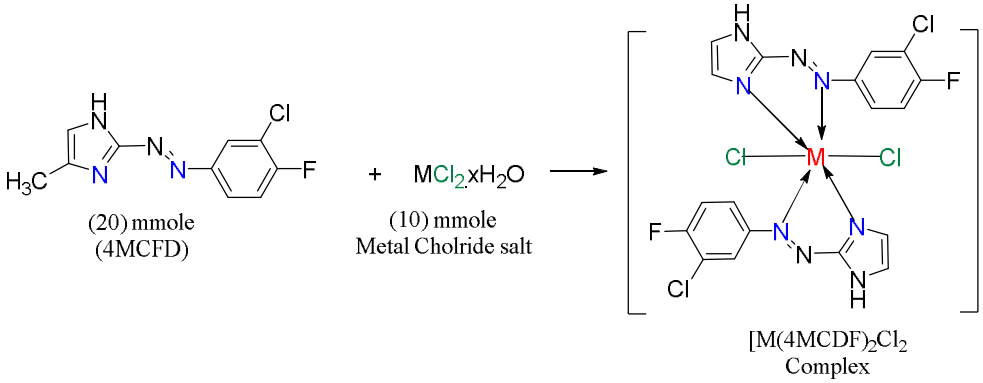

Scheme 2. Synthesis equation of (4MCFD) complexes.

Calculation of Stability Constants of the complexes:

Stability constants of the synthesized complexes calculated according the following equations at 10^{-4} M:

$$M + nL \leftrightarrow MLn \qquad (1)$$

$$\alpha \quad n\,\alpha C \quad 1-\alpha$$

M: Metal ion;

n: No. of coordinated ligands;

L: Ligand;

α: Degree of dissociation;

C: Concentration of ligand.

$$K_{Staibilty} = \frac{[ML\ n]}{[M]\,[L]^n} \qquad (2)$$

$$K = \frac{1-\alpha}{4\alpha^2 C^3} \quad (3)$$

$$\alpha = \frac{Am - As}{As} \quad (4)$$

where: A_m is Value of the complex absorption in the Mole Ratio;

A_s is Value of the complex absorption with increasing ligand.

Studying the inhibition ability towards resistance bacteria

Agar well diffusion technique[13] was employed to study the antibacterial activity. Mueller-Hinton agar (MHA) was utilized as the testing medium for the in-vitro antibacterial evaluation of the newly synthesized compounds versus *E. coli, Klebsiella, P. aeruginosa, and S. aureus.* Using a micropipette, bacterial isolate suspensions were made to match the 0.5 McFarland standard, and they were sterilized for 1.5 hours at 121°C. Each drug was made at a concentration of 50 mg/mL through being dissolved in DMSO solvent, following which the solutions were placed onto the culture's wall and incubated for 24 hours at 37°C. By using DMSO as a reference, the inhibition zone is measured (mm), that measures the effectiveness of the inhibition.

Results and discussion

Mass Spectrum of (4MCFD) New ligand

In coordination chemistry, mass spectrometry is a fundamental evaluation technique used to ascertain the molecular weight and create metal complexes[14]. Moreover, the synthesis and purification of coordination complexes can benefit from the use of mass spectrometry to identify the existence of impurities or other substances in a sample. Mass spectrum of (4MCFD) ligand emerged the molecular peak at (m/z = 293) that is provided the molecular weight of this ligand, while the base beak appeared at (m/z = 121) which refers to the fragment $[C_5H_6ClF]^+$ that is formed from the fragment $[C_6H_3ClFN]^{+\cdot}$ after opening the benzene ring and losing (-NCH) atoms. The general fragmentation paths take two ways, the first one started by losing (-F), and ($-CH_3$) then followed by known loosing of ($-N_2$)

molecule in azo compounds at (m/z = 177), whereas the second path started by cleaving the azo bond in the (4MCFD) molecule[15] as shown in the figure 2 and scheme 3.

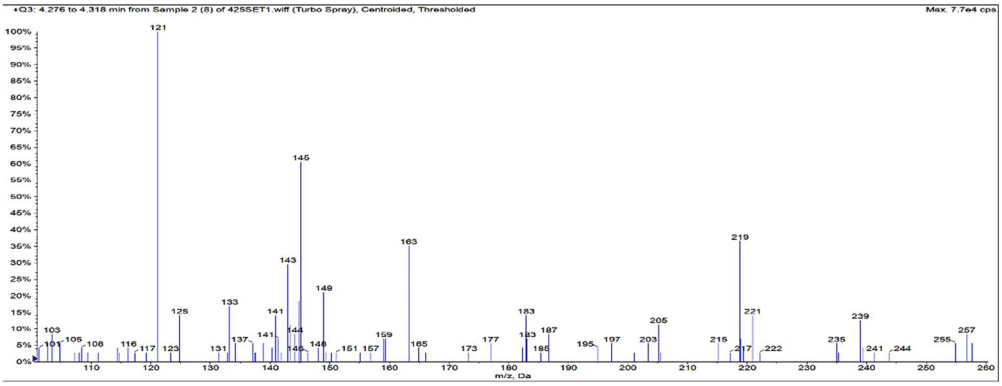

Figure 2. Mass spectrum of (4MCFD) ligand.

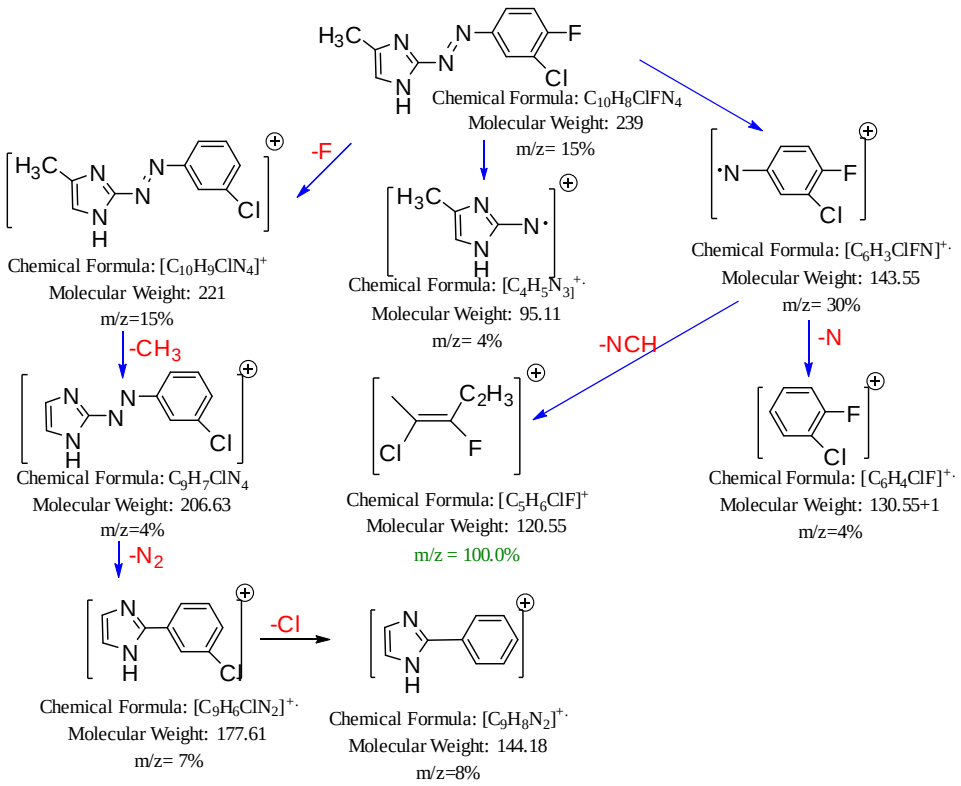

Scheme 3. Mass fragmentation of (4MCFD) ligand.

^{1}H-NMR and ^{13}C-NMR Spectra of (4MCFD) Ligand

Figure 3 shows ^{1}H-NMR spectrum of (4MCFD) ligand in DMSO-D6 solvent. The singlet signal of this solvent appeared at 2.52 ppm. The ligand exhibited (s, 3H,-CH_3) of substituted methyl group on the imidazole hetrocyclic ring at 2.25 ppm, (m, Ar-H) at 7.42-7.86 ppm for imidazole and benzene rings, while singlet signal of the proton that bonded to (N1) atom of imidazole (s, 1H, imdazole) at 12.70 ppm. These values of signals supported the type, and position of protons in this ligand. ^{13}C-NMR spectrum by using DMSO-d6 as a solvent showed the signals of that solvent between 31.52-40.75 ppm. The signal of the carbon atom from methyl group apeared at 31.38 ppm, while aromatic carbon atoms appeared in between 122.85-151.32 ppm, these values also indicated the number, the type, and the location of carbon atoms inside the molecule as shown in the figure 4.

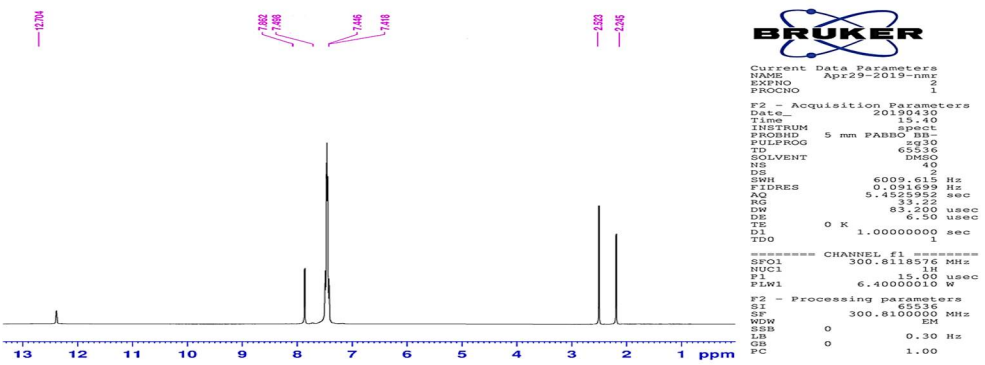

Figure 3. ^{1}H-NMR Spectrum of (4MCFD) ligand.

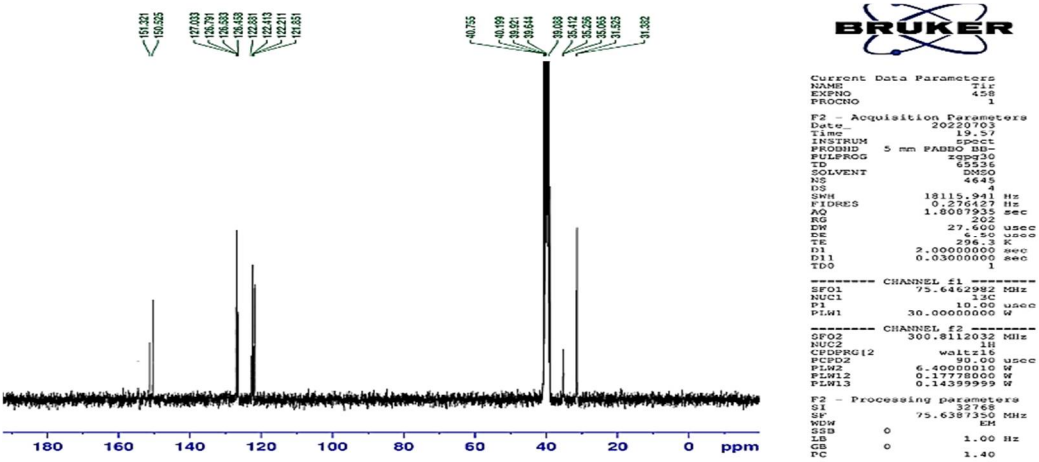

Figure 4. ^{13}C-NMR spectrum of (4MCFD) ligand.

Elemental analysis, and molar conductivity of (4MCFD) new ligand and complexes

Solid-purified complexes at stoichiometry ratio [1 : 2] [M:(4MCFD)] showed complete solubility in most organic solvents like MeOH, EtOH, DMF, DMSO, and $(CH_3)_2CO$. The Elemental Analysis (C.H.N.) of the (4MCFD) ligand and the synthesized complexes have shown excellent agreement between their theoretically calculated and experimental values that provided their molecular formulas. The values of Molecular Conductivity for 10^{-3} M for complexes in both of ethanolic and DMSO solvents showed non-electrolyte property[16,17] and there is clear different in both of colour and melting point of the ligand and the complexes, as shown in table 1.

Table 1. Several of the physicochemical characteristics for (4MCFD) and its solid purified complexes.

Compound	Molar conductivity ($S \cdot cm^2 \cdot mol^{-1}$)		M.P.	Color	Elemental analysis % calculated (Found)		
	Ethanol	DMSO			C	H	N
(4MCFD)	-------	---------	171-173	Orange	50.33 (50.30)	3.38 (3.40)	23.48 (23.49)
$[Co(L)_2Cl_2]$	15.4	13.7	232-234	Brown	37.33 (37.30)	2.09 (2.04)	19.35 (19.39)
$[Ni(L)_2Cl_2]$	15.1	13.3	238-240	Brown	37.35 (37.36)	2.09 (2.09)	19.36 (19.40)
$[Cu(L)_2Cl_2$	17.3	14.6	244-247	Purple	37.04 (37.07)	2.07 (2.10)	19.20 (19.22)
$[Cd(L)_2Cl_2]$	16.8	13.5	253-255	Red	34.18 (34.16)	1.91 (1.92)	17.71 (17.75)
$[Hg(L)_2Cl_2]$	17.5	14.3	267-270	Red	30.00 (30.06)	1.68 (1.66)	15.55 (15.62)

L: (4MCFD) ligand

Spectra of (4MCFD) new ligand and it's complexes

Electronic Spectra of (4MCFD) appeared two peaks at 204, and 241 nm due to (π-π*) transitions of aromatic rings, which showed red shift in the complexes spectra as a result of electronic effecting after the coordination, also the peaks at 356, and 385 nm for (n-π*) of azoimine, and azo group, as well as intra ligand charge transfer (ILCT) for (4MCFD) showed noticeable shifting to the high values of wavelength in the complexes spectra after the coordination as shown in table 2 and figure 5.

Table 2. Types of electronic transitions of (4MCFD) and complexes in ethanol solvent at 25 °C.

Compound	Wavelength (nm)	Type of transitions
(4MCFD)	204, 241	π-π*
	356	n-π*
	385	ILCT
$[Co(4MCFD)_2Cl_2]$	224, 286	π-π*
	370	n-π*
	468	MLCT
$[Ni(4MCFD)_2Cl_2]$	224,288	π-π*
	372	n-π*
	494	MLCT
$[Cu(4MCFD)_2Cl_2]$	232,286	π-π*
	375	n-π*
	500	MLCT
$[Cd(4MCFD)_2Cl_2]$	236,288	π-π*
	380	n-π*
	488	MLCT
$[Hg(4MCFD)_2Cl_2]$	224,288	π-π*
	386	n-π*
	504	MLCT

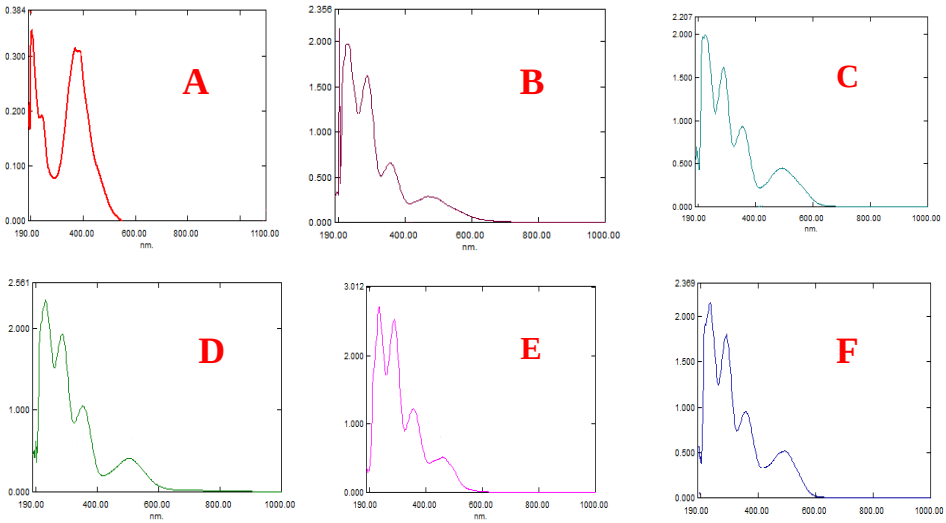

Figure 5. UV-Vis spectra of: A-(4MCFD); B-$[Co(4MCFD)_2Cl_2]$; C-$[Ni(4MCFD)_2Cl_2]$; D-$[Cu(4MCFD)_2Cl_2]$; E-$[Cd(4MCFD)_2Cl_2]$; F-$[Hg(4MCFD)_2Cl_2]$.

FT-IR Spectra of (4MCFD) new ligand and it's complexes

FT-IR spectrum of (4MCFD) showed *ν*(C=N) and *ν*(C-N) of imidazole ring[19,20] at 1583 cm^{-1} and 1273 cm^{-1} which appeared noticeable changes in the complexes spectra because of participation of imidazole heterocyclic ring in the coordination. The wavenumber of *ν*(N=N)[21-26] apeared at 1487 cm^{-1}, this group also exhibited shifting in position in the complexe's spectra which confirms the contribution of this group on the interaction with metal ion, as described in figure 6 and table 3.

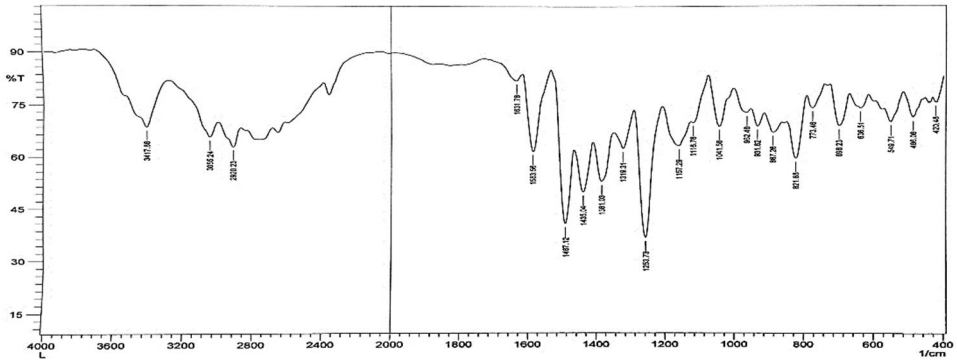

Figure 6. FT-IR spectrum of (4MCFD) ligand.

Table 3. Wavenumber values of FT-IR spectrum of (4MCFD) and the complexes.

The compound	***ν*(C=N) imidazole**	***ν* (C-N) imidazole**	***ν* (N=N)**	***ν* (M-N)**
(4MCFD)	1583 m	1273 s	1487 s	-----
$[Co(4MCFD)_2Cl_2]$	1556 m	1264 s	1468 s	473 w
$[Ni(4MCFD)_2Cl_2]$	1554 m	1260 s	1463 s	471 w
$[Cu(4MCFD)_2Cl_2]$	1567 m	1255 m	1456 m	465 w
$[Cd(4MCFD)_2Cl_2]$	1560 m	1252 m	1450 m	461 w
$[Hg(4MCFD)_2Cl_2]$	1563 m	1250 m	1447 m	455 w

Effecting of (pH) value of the complexation

Effect of pH medium on complexation process was studied for all complexes at a concentration of 0.5×10^{-4} M at range of buffer solutions between (4 - 9.5) at 25 ^{o}C, all of the complexes showed optimum complexation at 7.5 pH for Cobalt(II), Nickel(II), and Copper(II) complexes, and pH = 8.0 for Cadmium (II), and Mercury (II) complexes due to the nature of imidazole ring, and absence of acidic functional groups, as shown in figure 7.

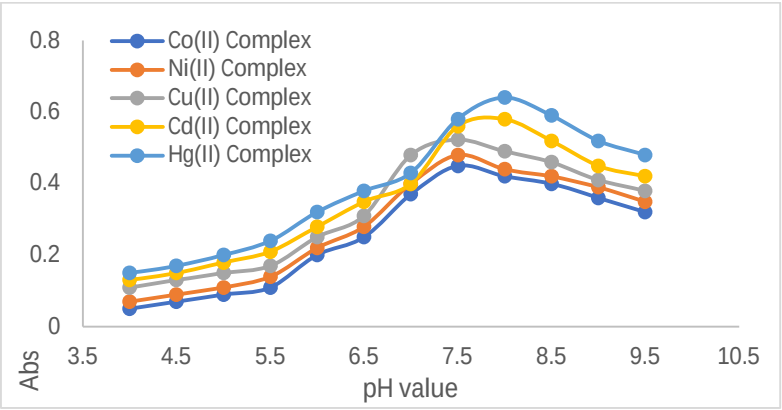

Figure 7. pH Curves of (4MCFD) complexes.

Magnetic susceptibility of (4MCFD) complexes

Magnetic susceptibility values for the complexes showed diamagnetic behaviour for Cd(II), and Hg(II) complexes, revealing an electronic configuration ($t_2g^6eg^4$) of these divalent ions, while 4.65 B.M of Co(II) complex due to three unpaired electrons supported ($t_2g^5eg^2$) of the distorted octahedral shape of this complex. The value 2.80 B.M of Ni(II) complex supported the presence of two unpaired electrons of the outer shell which have a ($t_2g^6eg^2$) for an octahedral geometry. Finally, the value 1.73 B.M for Cu(II) complex indicated the distorted octahedral geometry for one electron of the outer shell of copper central metal ion.

Stability constants of the complexes

Value of stability constants at the (1 : 2) molar ratio (M:4MCFD) explained that all of the prepared complexes have a high stability; as well as these values agreed with Irving-Williams for the first serious of transition metal divalent ion complexes, as shown in the table 4.

Table 4. Values of (Am), (As), α, K (stability), and log (K) of the complexes

Compound (M:L)(1:2)	Am	As	α	K($mol^{-1} \cdot L^2$)	Log K
$[Co(4MCFD)_2Cl_2]$	0.36	0.39	-0.076	455000	5.658
$[Ni(4MCFD)_2Cl_2]$	0.39	0.43	-0.093	315932.4	5.490
$[Cu(4MCFD)_2Cl_2]$	0.48	0.50	-0.040	1625000	6.210
$[Cd(4MCFD)_2Cl_2]$	0.52	0.55	-0.054	886111.1	5.947
$[Hg(4MCFD)_2Cl_2]$	0.56	0.58	-0.0344	2175000	6.337

Geometrical shapes of the complexes

The octahedral geometry in all of the complexes was suggested according to previous measurements. The coordination of both (4MCFD) molecules with each of the central metal ions occurs through two chelate sites, the first one being nitrogen atom (N3) of the imidazole ring, and the other being one of the nitrogen atoms of the azo group. The other two positions were occupied by chloride ion ligands, as seen in figure 8.

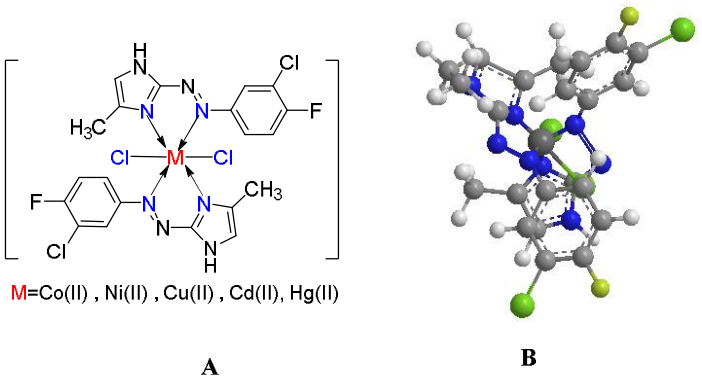

Figure 8. A: Geometrical structure of (4MCFD) complexes; **B:** 3D Theoretical suggested structure of (4MCFD) complexes drawing by Chem Office program.

The inhibition zones were measured for (50) ppm of the (4MCFD) and the complexes versus four distinct types of bacteria *(E. coli, P. aeruginosa, K. pneumonia,* and *S. aureus),* generally *S. aureus* showed more resistance comparing the other studied bacteria due to the differences of their cell membrane's structure. gram-positive bacteria have a peptidoglycan coating that shields them from antibiotics, whereas gram-negative bacteria have an outer membrane and a weaker peptidoglycan layer, making them more sensitive to these chemicals. The inhibition values of bacteria (as shown in figures 9-13) are graded in the following order:

K. pneumonia >E. coli > P. aeruginosa, >S. aureus

The majority of studies have indicated that the metal complexes can become more active than free ligand. Chelation theory can be used to explain why metal complexes have increased activity by exchanging positive charges with the donor atoms in the ligands, chelation reduces the polarity of the metal ion, and it may result in π-electron delocalization, because of this behavior, the metal chelate has a stronger lipophilic nature, which makes it easier for it to enter through the lipoid layer of the microbe and kill it.[3] Other parameters like as the metal's solubility, conductivity, and length of the bond with its ligand also increase activity.[27] In spite of the fact that the specific antibacterial action's biochemical mechanism is unidentified, microbes may include a range of targets. Inhibition of cell wall production causes increased cell permeability (or) lipoprotein disarray causes cell death.

Normal cellular processes are interfered with as a result of denaturation of one or more proteins in the cell. Azomethine group formation with the active site of a cell component results in an interference

with regular cellular functions. These complexes have a few donor atoms that haven't been coordinated which can form bonds with the trace elements in microbes to increase their activity. Pairing this with the uncoordinated site might prevent microbial development.

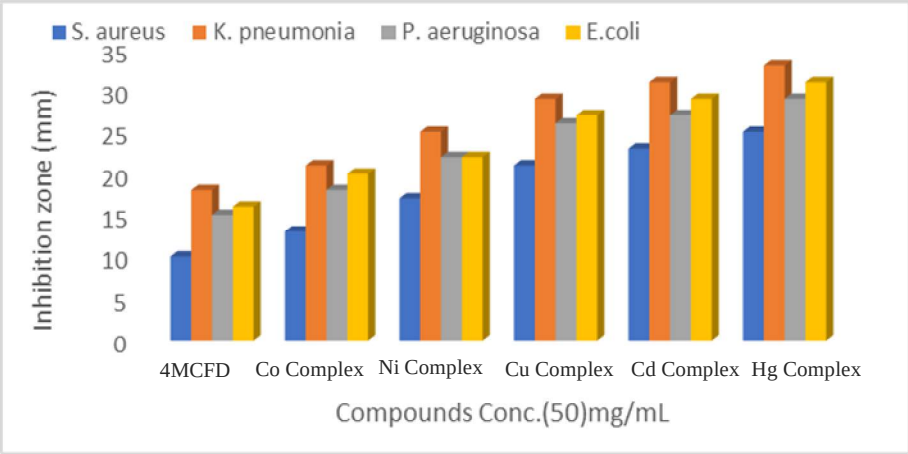

Figure 9. (4MCFD) and complexes inhibitory activity.

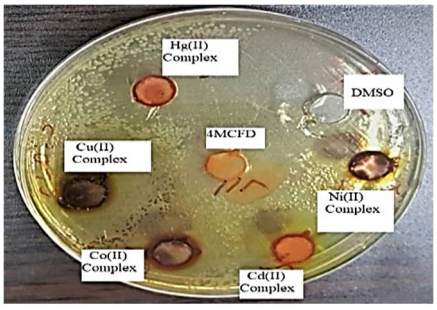

Figure 10. Inhibition ability of *K. pneumonia.*

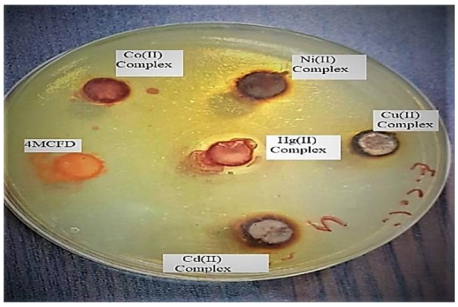

Figure 11. Inhibition ability of *E. coli.*

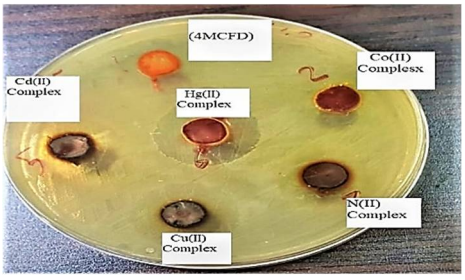

Figure 12. Inhibition ability of *P. aeruginosa*.

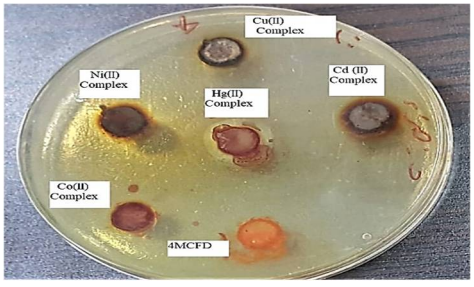

Figure 13. Inhibition ability of *S. aureus.*

Conclusions

(4MCFD) new compound and its octahedral synthesized complexes with various transition ions were prepared with high yield, purity, stability, and colorimetric sensitivity. These synthesized compounds showed good bacterial inhibitory capacity especially towards Gram-negative bacteria due to the ability of donor atoms to develop bonds with trace elements in microorganisms to enhance their activity, and the higher lipophilicity of metal chelate.

References

1. Mgheer, T. H.; Abdulmahdi, B. S.; Mohammed, L. A. Bio-Chemical study and preparation of some new mixed ligand complexes with novel(azo) ligand derived from 5-methyl imidazole and 1,10-phenanthroline compounds. *J. Pharm. Negat.* **2020**, *13(7)*, 7135–7146.
2. Ward, H. A.; Musa, T. M.; Nasif, Z.N. Synthesis and characterization of some transition metals complexes with new ligand azo imidazole derivative. *Al-MJS*. **2022**, *33(2)*, 31–38.
3. Witwit, I. N.; Mubark, H. M. H.; Ali, A. A. M. Synthesis and studying the coordination behavior of a new heterocyclic imidazole azo ligand with some of the first series transition and (IIB) ions. *AIP Conf. Proc*. **2020**, *2290*, 030025.
4. Slassi, S. Aarjane, M.; El-Ghayoury, A.; Allain, A.; Amina, A. Synthesis, crystal structure, photoisomerization, and DFT studies of novel azo compounds based on imidazole. *J. Phys. Org. Chem*. **2023**, *36(5)*, e4486.
5. Mahmoud, W. A.; Ali, A. A. M.; Kareem, T. A. Preparation and spectral characterization of new azo imidazole ligand 2-[(2`-cyanophenyl)azo]-4,5-diphenyl imidazole and its complexes with Co(II), Ni(II), Cu(II), Zn(II), Cd(II) and Hg (II) ions. *Baghdad Sci. J*. **2015**, *12(1)*, 96–109.
6. Mezgebe, K.; Mulugeta, E. Synthesis and pharmacological activities of azo dye derivatives incorporating heterocyclic scaffolds: a review. *RSC Adv*. 2022, 12(40), 25932–25946.
7. Ribeiro, A. I.; Vieira, B.; Dantas, D.; Silva, B.; Pinto, E.; Cerquera, F.; Silva, R.; Remião, F.; Padrão, J.; Dias, A. M.; Zille, A. Synergistic antimicrobial activity of silver nanoparticles with an emergent class of azoimidazoles. *Pharmaceutics* **2023**, *15(3*), 926.

8. Atiya, R. N.; Razzaq, Z. L.;Yahya, W. I.; Neamah, H. M. Synthesis, characterization and studying biological activity of heterocyclic compounds. *Int. J. Drug Deliv. Technol.* **2023**, *13(01*), 205–211.

9. Romero, D. H.; Torres Heredia, V. E.; García-Barradas, O.; Marquez Lopez, M. A.; Sanchez Pavon, E. Synthesis of imidazole derivatives and their biological activities. *J. Chem. Biochem*. **2014**, *2(2)*, 45**–**83.

10. Sen, C.; Patra, C.; Mondal, S.; Datta, A.; Mallick, D.; Mondal, T.; Askun, T.; Celikboyun, P.; Canturk, Z.; Sinha, C. Platinum(II)-azoimidazole drugs against TB and cancer: structural studies, cytotoxicity and anti-mycobacterial activity. *Polyhedron* **2018**, *152*, 1–10.

11. Chhetri, A.; Chhetri, S.; Rai, P.; Sinha, B.; Brahman, D. Exploration of inhibitory action of azo imidazole derivatives against COVID-19 main protease (M^{pro}): A computational study. *J. Mol. Struct*. **2021**, *1224*, 129178.

12. Chhetri, A.; Chhetri, S.; Rai, P.; Mishra, D.; Sinha, B.; Brahman, D. Synthesis, characterization and computational study on potential inhibitory action of novel azo imidazole derivatives against COVID-19 main protease (M^{pro}: 6LU7). *J. Mol. Struct*. **2021**, *1225*, 129230.

13. Balouiri, M.; Sadiki, M.; Ibnsouda, S. K. Methods for in vitro evaluating antimicrobial activity: A review. *J. Pharm. Anal*. **2016**, *6(2)*, 71–79.

14. Henderson, W.; McIndoe, J. S. Mass Spectrometry of Inorganic, Coordination and organometallic compounds: tools - techniques - tips. John Wiley & Sons, Ltd. **2005**, 127–132.

15. Kyhoiesh, H. A. K.; Al-Hussainawy, M. K.; Waheeb, A. S.; Al-Adilee, K. J. Synthesis, spectral characterization, lethal dose (LD50) and acute toxicity studies of 1,4-bis(imidazolylazo)benzene (BIAB). *Heliyon* **2021**, *7(9)*, e07969.

16. Sieber, M. A.; Lengsfeld, P.; Walter, J.; Schirmer, H.; Frenzel, T.; Siegmund, F.; Weinmann, H.-J.; Pietsch, H. Gadolinium-based contrast agents and their potential role in the pathogenesis of nephrogenic systemic fibrosis: the role of excess ligand. *J. Magn. Reason. Imaging.* **2008**, *27*, 955–962.

17. Kareem, I. K.; Waddai, F. Y.; Abass, G. J. Synthesis, Characterization and biological activity of some transition metal complexes with new Schiff base ligand type (NNO) derivative from benzoin. *J. Pharm. Sci. Res.* **2019**, *11(1)*, 119–124.

18. Ali, F. J.; Al-Ameri, L. A. M.; Ali, A. M. Synthesis and identification and biological studies of new azo dyes derived from imidazole and their chelate complexes. *Indian J. Med. Forensic Med. Toxicol*. **2021**, *15(2)*, 1253–1260.

19. Fekri, L. Z.; Nateghi-Sabet, M. Synthesis of new azo-dispersive dyes with benzo[d]imidazole moiety and new bis benzo[d]imidazoles using DABCO-diacetate as a green media. *J. Chin. Chem. Soc.* **2020**, *68(4)*, 695–703.

20. Chen, S. S. The roles of imidazole ligands in coordination supramolecular systems. *CrystEngComm*. **2016**, *18(35)*, 6543–6565.

21. Slassi, S.; Fix-Tailler, A.; Larcher, G.; Amine, A.; El-Ghayoury, A. Imidazole and azo-based Schiff bases ligands as highly active antifungal and antioxidant components. *Heteroatom Chem*. **2019**, 6862170.

22. Kılınçarslan, R.; Erdem, E.; Kocaokutgen, H. Synthesis and spectral characterization of some new azo dyes and their metal complexes. *Transition Met. Chem.* **2007**, *32(1)*, 102–106.

23. Alabidi, H. M.; Alabidi, A. M.; Makki, N. F. Synthesis and spectroscopic studying of new azo ligand from 2-naphthol derivative and it's complexes with some transition metal ions. *QJPS.* **2018**, *23(1)*, 186–195.

24. Mandour, H. S.; Abouel-Enein, S. A.; Morsi, R. M. M.; Khorshed, L. A. Azo ligand as new corrosion inhibitor for cupper metal: Spectral, thermal studies and electrical conductivity of its novel transition metal complexes. *J. Mol. Struct.* **2021**, *1225*, 129159.

25. Waheeb, A. S.; Al-Adilee, K. J. Synthesis, characterization and antimicrobial activity studies of new heterocyclic azo dye derived from 2-amino- 4,5-dimethyl thiazole with some metal ions. *Mater. Today: Proc*. **2021**, *42(5)*, 2150–2163.

26. Abd El-wahaab, B.; Elgendy, K.; El-didamony, A. Synthesis and characterization of new azo-dye reagent and using to spectrophotometric determination of samarium (III) in some industrial and blood samples. *Chem. Pap*. **2020**, *74*, 1439–1448.

27. Li, M.; Zeng, M.; Zhang, H.; Chen, H.; Guan, L. Biological activity predictions of ligands based on hybrid molecular fingerprinting and ensemble learning. *ACS Omega.* **2023**, *8(6)*, 5561–5570.